Biochem. J. (2013) **449**, 459–468 (Printed in Great Britain) doi:10.1042/BJ20121360

Loss of LSD1 (lysine-specific demethylase 1) suppresses growth and alters gene expression of human colon cancer cells in a p53- and DNMT1 (DNA methyltransferase 1)-independent manner

Lihua JIN*, Christin L. HANIGAN*, Yu WU*, Wei WANG*†, Ben Ho PARK*, Patrick M. WOSTER‡ and Robert A. CASERO, Jr*[1]

*The Sidney Kimmel Comprehensive Cancer Center at Johns Hopkins, The Johns Hopkins University School of Medicine, Baltimore, MD 21287, U.S.A., †Predoctoral Training Program in Human Genetics, The Johns Hopkins University School of Medicine, Baltimore, MD 21287, U.S.A., and ‡Department of Drug Discovery and Biomedical Sciences, The Medical University of South Carolina, Charleston, SC 29425, U.S.A.

Epigenetic silencing of gene expression is important in cancer. Aberrant DNA CpG island hypermethylation and histone modifications are involved in the aberrant silencing of tumour-suppressor genes. LSD1 (lysine-specific demethylase 1) is a H3K4 (histone H3 Lys[4]) demethylase associated with gene repression and is overexpressed in multiple cancer types. LSD1 has also been implicated in targeting p53 and DNMT1 (DNA methyltransferase 1), with data suggesting that the demethylating activity of LSD1 on these proteins is necessary for their stabilization. To examine the role of LSD1 we generated LSD1 heterozygous (*LSD1*$^{+/-}$) and homozygous (*LSD1*$^{-/-}$) knockouts in the human colorectal cancer cell line HCT116. The deletion of LSD1 led to a reduced cell proliferation both *in vitro* and *in vivo*. Surprisingly, the knockout of LSD1 in HCT116 cells did not result in global increases in its histone substrate H3K4me2 (dimethyl-H3K4) or changes in the stability or function of p53 or DNMT1. However, there was a significant difference in gene expression between cells containing LSD1 and those null for LSD1. The results of the present study suggested that LSD1 is critical in the regulation of cell proliferation, but also indicated that LSD1 is not an absolute requirement for the stabilization of either p53 or DNMT1.

Key words: chromatin, epigenetics, FAD-dependent oxidase, histone modification, transcriptional repression.

INTRODUCTION

The term ‘epigenetic’ refers to heritable changes regulating gene expression that are not a result of changes in the primary DNA sequence. In cancer, aberrant epigenetic silencing of tumour-suppressor genes is a common occurrence that is associated with abnormal DNA methylation patterns and changes in covalent histone modifications [1]. These histone modifications, including acetylation, methylation and phosphorylation, play major roles in the regulation of chromatin structure and gene transcription [1], with each modification having a context-dependent association with transcriptional activation or repression. For example, H3K4 (histone H3 Lys[4]) methylation is associated with transcriptional activation, whereas H3K9 (histone H3 Lys[9]) methylation is associated with transcriptional repression. Histone methylation is catalysed by HMTs (histone methyltransferases), and methyl marks are removed by the catalytic activity of enzymes such as the FAD-dependent LSDs (lysine-specific demethylases) LSD1 and LSD2 [2–4] and the Jumonji C domain-containing histone demethylases [5]. Structural studies have shown that LSD1 has three major domains: an N-terminal SWIRM (Swi3p/Rsc8p/Moira) domain, a C-terminal AOL (amine oxidase-like) domain and a central protruding Tower domain [6–8]. The C-terminal domain has a significantly high sequence homology to the polyamine oxidases that belong to the FAD-dependent enzyme family [2,9]. The Tower domain represents a binding surface for the LSD1 co-repressor partner protein CoREST [REST (RE1-silencing transcription factor) corepressor 1]. HDACs (histone deacetylases), including HDAC1 and HDAC2, have also been demonstrated to be members of some LSD1 core complexes. HDAC activity deacetylates histone H3 lysine residues, which permits the binding of CoREST to the nucleosome [10]. Furthermore, the SWIRM domain makes close interactions with the AOL domain, forming a highly conserved cleft, which may serve as an additional histone tail-binding site [6,10,11]. LSD1 demethylates H3K4me2 (dimethyl)/H3K4me1 (monomethyl) through an oxidative reaction that leads to the reduction of the protein-bound FAD cofactor and the production of H_2O_2 and formaldehyde [12].

The activity of LSD1 has been proposed to be essential for mammalian development and has been implicated in many important cellular processes, including proliferation, differentiation, haematopoiesis, adipogenesis, maintenance of DNA methylation and tumorigenesis [13–22]. Through interactions with various transcription factors including the AR (androgen receptor) [23,24], ER (oestrogen receptor) [25] and co-repressor complexes, LSD1 impacts transcription by demethylating H3K4. Further, LSD1 has been suggested to demethylate H3K9 and non-histone substrates such as p53 and DNMT1 (DNA methyltransferase 1) [13,18,26]. It has been reported that DNMT1 can be methylated by SET7/9 (SET domain-containing histone methyltransferase 7/9) and

Abbreviations used: AAV, adeno-associated viral; AOL, amine oxidase-like; ATRA, all-*trans* retinoic acid; ChIP, chromatin immunoprecipitation; COBRA, combined bisulfite restriction analysis; CoREST, RE1-silencing transcription factor corepressor 1; DNMT1, DNA methyltransferase 1; ES, embryonic stem; GAPDH, glyceraldehyde-3-phosphate dehydrogenase; HA, homology arm; HDAC, histone deacetylase; HEK, human embryonic kidney; H3K4, histone H3 Lys[4]; H3K9, histone H3 Lys[9]; H3K9ac, H3K9 acetylation; JARID1, Jumonji, AT rich interactive domain 1; LINE-1, long interspersed nucleotide element 1; LSD, lysine-specific demethylase; me1, monomethyl; me2, dimethyl; me3, trimethyl; pAAV, AAV plasmid; PCNA, proliferating cell nuclear antigen; qPCR, quantitative PCR; SEPT, synthetic exon promoter trap; SET7/9, SET domain-containing histone methyltransferase 7/9; SWIRM, Swi3p/Rsc8p/Moira; TSS, transcriptional start site; VAT1L, vesicle amine transport protein 1 homologue-like; VIM, vimentin.

[1] To whom correspondence should be addressed (email rcasero@jhmi.edu).

demethylated by LSD1 *in vitro*. Loss of LSD1 in ES (embryonic stem) cells induces a progressive loss of DNA methylation that correlates with a decrease in DNMT1 protein resulting from reduced DNMT1 stability [13]. Furthermore, LSD1 has been implicated in the demethylation of K370me2 (dimethylated Lys^{370}) of p53. This proposed demethylation is thought to cause inactivation of p53 by inhibiting both the ability of p53 to bind to DNA and its association with 53BP1 (p53-binding protein 1) [26]. In addition, it has been suggested that LSD1 deficiency delays the p53 stabilization that is induced by DNA damage, leading to a delayed induction of p21 [18]. These results implicated LSD1 as an oncoprotein by inactivating p53, consistent with the fact that LSD1 is overexpressed in various human tumours [25,27–31].

To identify LSD1 targets and further our understanding of the role of LSD1 in tumorigenesis, we have generated LSD1 heterozygous (*LSD1*$^{+/-}$) and homozygous (*LSD1*$^{-/-}$) knockouts in the human colorectal cancer cell line HCT116. The results indicate that the loss of LSD1 leads to a significant increase in the expression of several genes, consistent with its proposed role as a transcriptional repressor. Surprisingly, the loss of LSD1 had no effect on the cellular levels of either p53 or DNMT1, suggesting that the stability of these proteins is not dependent on LSD1 activity. Finally, microarray data analyses have identified a number of genes whose expression is dependent upon LSD1. Therefore, these *LSD1*-knockout cell lines provide unique tools for the identification of the specific targets of LSD1 and the development of strategies to target the function of the enzyme in tumours.

MATERIALS AND METHODS

Construction of the AAV (adeno-associated viral) targeting vector

Targeted knockout of the *LSD1* gene was conducted with a pAAV (AAV plasmid) vector as described previously [32,33]. The generation scheme of the pAAV-based targeting vector is shown in Supplementary Figure S1 (at http://www.biochemj.org/bj/449/bj4490459add.htm). HCT116 genomic DNA was used as the template for generating the HAs (homology arms) for gene targeting. Each primer contained a unique restriction enzyme site at its 5′-end. The restriction enzyme sites allowed cloning of HA1 and HA2 into the pSEPT vector. The two HAs flanked a SEPT (synthetic exon promoter trap) element featuring a selection marker gene that was surrounded by two LoxP sites. These LoxP sites facilitated the removal of the selection marker element by transient expression of the *Cre* recombinase. The final construct was assembled by ligation of the NotI sites and includes the two HAs, the SEPT/LoxP cassette and a pAAV shuttle vector that contains AAV ITRs (inverted terminal repeats). The primer sequences used for the PCRs are shown in Supplementary Table S1 (at http://www.biochemj.org/bj/449/bj4490459add.htm).

Generation of LSD1 knockouts in HCT116 cells

HCT116 cells were maintained in McCoy's 5A medium with 10 % FBS (fetal bovine serum) and grown at 37 °C in a 5 % CO_2 atmosphere. Fugene transfection reagent (Promega) was used to co-transfect HEK (human embryonic kidney)-293 cells with the recombinant construct pAAV-RC and pHelper virus to establish AAV particles. The HEK-293 cells then underwent three freeze–thaw cycles to release the viral particles for infection into wild-type HCT116 cells. For infection with virus, HCT116 cells were grown in T-75 flasks to ~70 % confluence, the AAV particles were added (500 μl into 4 ml of growth medium) and the cells were incubated at 37 °C for 4 h. Additional medium was then added to a total of 12 ml, the cells were allowed to grow for 48 h, harvested by trypsinization and then distributed into 96-well plates containing neomycin (0.5 mg/ml) selection medium. Neomycin-resistant colonies were expanded, replicated and pooled. PCR-based screening was used to identify the presence of cells that had undergone homologous integration of the targeting vectors, followed by PCR screening of individual colonies isolated from these positive pools, as described previously [33]. Targeted cells were then infected with an adenovirus encoding *Cre* recombinase to remove the selection cassette, followed by single-cell dilution and screening by PCR to confirm *Cre* recombination. The primer sequences used for the PCRs are shown in Supplementary Table S1.

Western blotting

The cytoplasmic and nuclear fractions were prepared for Western blot analysis using the NE-PER Nuclear and Cytoplasmic Extraction kit (Pierce). Primary antibodies against LSD1, JARID1 (Jumonji, AT rich interactive domain 1) A and SET7/9 were from Cell Signaling Technology, and antibodies against H3K4me1/2, H3K9me2, HDAC1, HDAC2 and CoREST were from Millipore. Primary antibodies against LSD2, JARID1B and histone H3 were from Abcam and the antibody against DNMT1 was from Sigma. The anti-PCNA (proliferating cell nuclear antigen) monoclonal antibody was purchased from Calbiochem. Dye-conjugated fluorescent secondary antibodies were used to quantify the Western blotting results using the Odyssey Infrared Detection system and software (LI-COR Biosciences).

To test whether the DNA damage response of p53 was altered by the loss of LSD1, 8.0×10^5 cells were seeded in 10-cm dishes, incubated for 48 h and then treated with 1 μM doxorubicin (Invitrogen) for 8 and 24 h. The cells were washed with ice-cold PBS, harvested and lysed in RIPA buffer [150 mM NaCl, 50 mM Tris/HCl (pH 7.2), 0.5 % Nonidet P40, 1 % Triton X-100 and 1 % sodium deoxycholate] containing an EDTA-free protease inhibitor cocktail (Pierce). Total protein was analysed using antibodies against p53 (1:1000 dilution; Cell Signaling Technology), p21 (1:1000 dilution; BD Pharmingen) and actin (1:2000 dilution; Santa Cruz Biotechnology). Dye-conjugated secondary antibodies were used to quantify Western blotting results using the Odyssey Infrared Detection system and software.

COBRA (combined bisulfite restriction analysis) assay

Methylation of the LINE-1 (long interspersed nucleotide element 1) promoter was investigated using the COBRA assay as described previously [34]. Genomic DNA from cells was bisulfite modified using the EZ DNA Methylation kit (Zymo Research). PCR was then carried out with Platinum Taq polymerase (Invitrogen), using the bisulfite-modified genomic DNA as the template. The primers for amplification were 5′-TTGAGTTGTGGTGGGTTTTATTTAG-3′ (forward) and 5′-TCATCTCACTAAAAAATACCAAACA-3′ (reverse). The PCR products were purified, digested with the HinfI restriction enzyme, separated by electrophoresis on 6 % polyacrylamide gels and visualized by staining with ethidium bromide.

Cell proliferation and cell-cycle analysis

To determine the cell growth rate, 7.5×10^5 cells were seeded in T-25 flasks. At the indicated time points the cells were collected and counted using a T10 Automated Cell Counter (Bio-Rad Laboratories). For DNA histogram analysis, 7.5×10^5 cells were seeded in T-25 flasks and followed for 3 days. Cells

were collected, stained with propidium iodide and analysed using FACS.

Xenograft growth assay

Female athymic nude mice, obtained at 4–6 weeks-of-age (Harlan), received subcutaneous flank injections of suspensions containing 1.0×10^7 cells of the indicated genotype in 100 μl of Hanks buffered saline solution (BD Biosciences). Tumour measurements were initiated 10 days after implantation and measured twice weekly for 7 weeks. The NIH guide for the care and use of laboratory animals were followed in all experiments.

RNA isolation and qPCR (quantitative PCR)

RNA was extracted using the TRIzol® reagent (Invitrogen). First-strand cDNA of HCT116 cells was synthesized using Superscript III reverse transcriptase with oligo$(dT)_{20}$ primers (Invitrogen). Quantitative PCR was performed in a MyiQ single-colour real-time PCR detection system (Bio-Rad Laboratories) using SYBR Green Super mix for iQ (Quanta BioSciences). The primer sequences used for qPCR are shown in Supplementary Table S1. The amplification conditions consisted of a 15 min denaturation step, followed by 40 cycles of denaturation at 95 °C for 30 s, annealing at the designated temperature for 30 s and extension at 72 °C for 30 s.

Microarray analysis

Total RNA was isolated from *LSD1*$^{-/-}$, *LSD1*$^{+/-}$ and parental HCT116 cells using the standard TRIzol® protocol to perform a comparative microarray analysis using an Illumina HumanHT-12 v4 Expression BeadChip platform (Illumina). Statistical analysis for microarray data was performed using R and BioConductor software (http://www.bioconductor.org/). Data were normalized by robust spline normalization after variance-stabilizing transformation provided by the lumi package [35,36]. Heat maps were generated using probes with coefficients of variation greater than 0.1.

ChIP (chromatin immunoprecipitation)

ChIP analysis was performed using Protein A and Protein G Dynabeads® (Invitrogen) as reported previously [37]. Cells were exposed to 1 % formaldehyde to cross-link the proteins and 2.0×10^6 cells were used for each ChIP assay. The antibodies against H3 and LSD1 were from Abcam and antibodies against H3K4me1, H3K4me2, H3K4me3 (trimethyl), H3K9ac (H3K9 acetylation), H3K9me2 and H3K9me3 were from Millipore. Quantitative ChIP was performed using qPCR on the MyiQ single-colour real-time PCR detection system using the enzyme master mix from Quanta. The primer sequences used for qPCR for ChIP are shown in Supplementary Table S1. Sheared genomic DNA was used as a positive control (input) and for the normalization of DNA immunoprecipitated by LSD1. DNA immunoprecipitated by the anti-H3 antibody was used for the normalization of histone H3 modifications.

RESULTS AND DISCUSSION

Generation of LSD1 heterozygous (*LSD1*$^{+/-}$) and homozygous (*LSD1*$^{-/-}$) knockouts in HCT116 cells

To investigate the functions of LSD1 and identify LSD1 target genes, we generated *LSD1* heterozygous and homozygous knockouts in the human colorectal cancer cell line HCT116. For the creation of null alleles, exon 2 of the *LSD1* gene was targeted using an AAV-based targeting vector (Figure 1A). In the targeting vector HA1 and HA2 flank the selectable marker (SEPT)/LoxP cassette, and a stop codon sequence (TAGATAACTGA) is incorporated into HA2. Upon homologous recombination the disruption of exon 2 results in a shift of the correct open reading frame in the SWIRM domain of LSD1, prior to the amine oxidase domain that is essential for catalytic activity. After infection with the targeting vector, drug-resistant clones were selected with G418 and single clones were isolated. PCR-based screening was used to identify the single clones that harboured recombinant alleles. Using primers A and B, only a recombinant allele will generate a PCR product (1.4 kb) because primer B anneals within the SEPT element (Figure 1B, I). After identification of the correctly targeted allele the SEPT element was excised using *Cre* recombinase and its removal was verified by the absence of a PCR product when using primers A and B (Figure 1B, II). This first round of gene targeting resulted in the generation of cell lines that only have a single copy of the wild-type LSD1 (heterozygous), with only one LoxP site flanked by HA1 and HA2. A second round of gene targeting was performed with the heterozygous clones to generate homozygous LSD1-null clones. Primer C anneals at the site flanking the proposed deletion and was paired with the outside primer (primer D) (Figure 1B, III). Primers C and D can amplify both alleles, however, the second targeted allele retains the SEPT element and generates a product that is 2-kb larger than that generated from the first excised allele (the size of the SEPT element; Figure 1B, III). Therefore the homozygous clones are distinguishable from the heterozygous clones by the two different sizes of PCR products. Once successful targeting of the second allele was confirmed a second round of *Cre* infection was used to remove the remaining SEPT element from the second allele.

To confirm that the targeting strategy was successful, Western blot analysis for the LSD1 protein and qPCR analysis for *LSD1* mRNA were performed (Figure 1C). As expected, genetic disruption of exon 2 resulted in the complete loss of LSD1 protein and mRNA in the homozygously deleted cells, whereas the heterozygous LSD1 cells did not demonstrate a significant change in protein expression.

The loss of LSD1 in HCT116 cells does not change the global levels of histone marks or non-histone protein substrates

LSD1 has been shown to demethylate H3K4me2, and possibly H3K9me2, but the loss of LSD1 in HCT116 cells did not affect the global levels of H3K4me2 or H3K9me2 (Figure 2A). The co-repressor CoREST, together with HDAC1 and HDAC2, are important binding partners of LSD1 at some promoters. To determine whether the loss of LSD1 resulted in global changes in the protein expression level of these binding partners, Western blot analyses were performed using the nuclear extracts from LSD1 homozygous (*LSD1*$^{-/-}$), heterozygous (*LSD1*$^{+/-}$) and parental HCT116 cells (Figure 2B). It has been reported that the conditional deletion of LSD1 in mouse ES cells resulted in a reduction in the level of CoREST protein expression and associated HDAC activity, resulting in a global increase in H3K56 acetylation, but no change in H3K4 methylation [15]. Consistent with these observations in ES cells, the HCT116 cells exhibited no change in global H3K4me2 levels after *LSD1* knockout (Figure 2A); however, in contrast with the ES cell results, no change in global CoREST levels were observed in the *LSD1*$^{-/-}$ cells (Figure 2B). This different expression pattern of

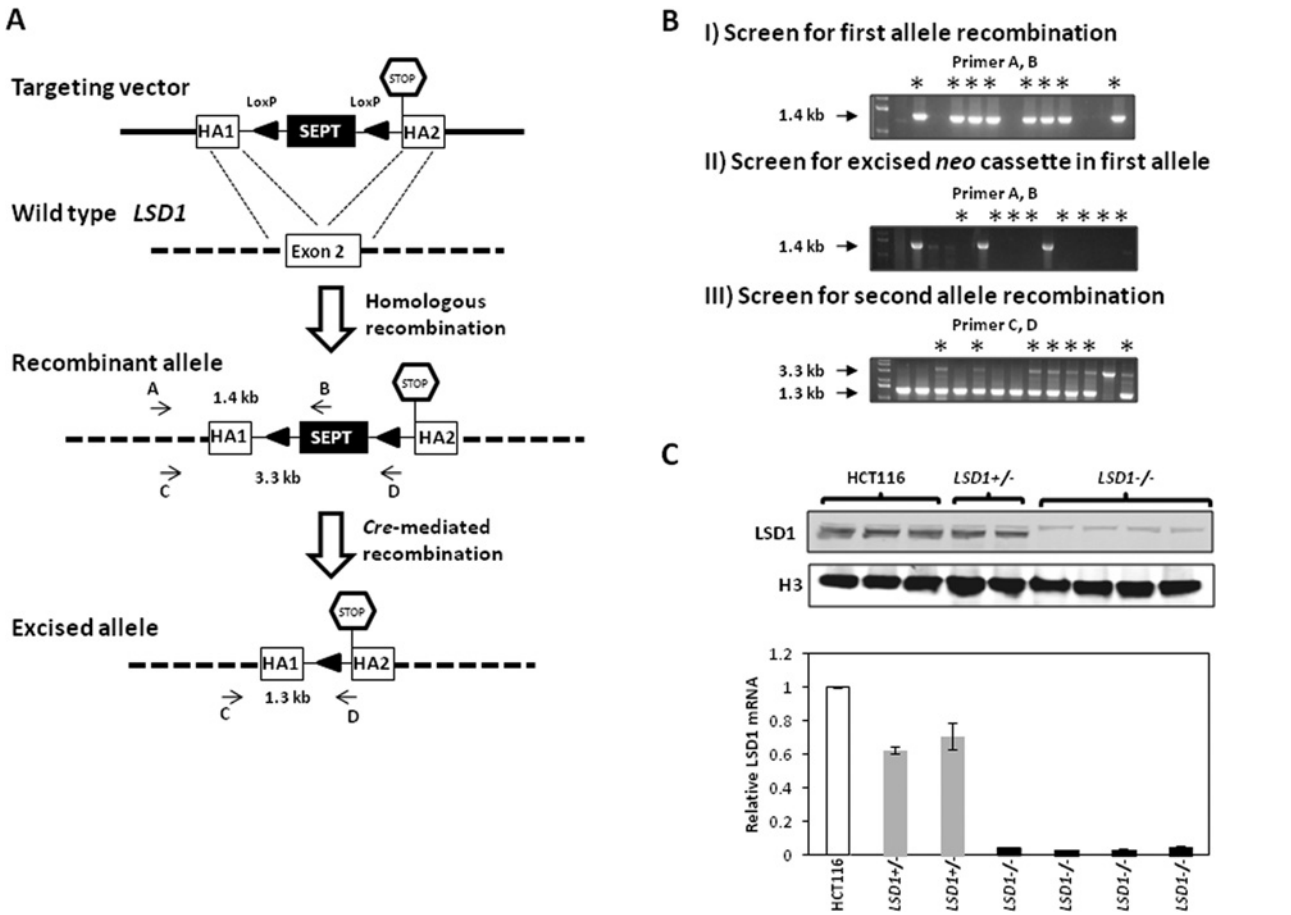

Figure 1 Generation of LSD1 heterozygous (*LSD1*$^{+/-}$) and homozygous (*LSD1*$^{-/-}$) knockouts in HCT116 cells

(**A**) The AAV-based targeting vector showing the two homology arms (HA1 and HA2) targeting exon 2 of the *LSD1* gene and flanking the SEPT/LoxP cassette. A stop codon was added to HA2. After the wild-type HCT116 cells were infected with viral particles, individual drug-resistant colonies were selected and PCR-based screening was done to identify colonies that had undergone homologous integration of the targeting vector. Transient expression of *Cre* recombinase was used to remove the selection cassette from the successfully recombined alleles, therefore restoring the sensitivity of the cells to drug selection and facilitating the targeting of the second allele. (**B**) First-round *LSD1* gene targeting in the wild-type HCT116 cells was performed to generate heterozygous cells (*LSD1*$^{+/-}$ cells). Primer A anneals outside of the homology region and primer B is within the SEPT element. Therefore only successful recombination will generate a 1.4-kb PCR product with primers A and B (I). PCR amplification using primers A and B was also used to identify clones from which the SEPT element has been successfully excised following *Cre*-mediated recombination. In this case, the alleles from which the SEPT element was removed did not generate 1.4-kb PCR products (II). The second round of gene targeting in *LSD1*$^{+/-}$ cells was performed to generate homozygous LSD1-null clones (*LSD1*$^{-/-}$ cells). Primer D anneals at the site flanking the proposed deletion and is paired with outside primer C. If homologous recombination successfully occurs in the second allele, primers C and D can amplify both alleles. However, the second targeted allele retains the SEPT element and generates a product that is 2-kb larger than that generated from the first excised allele (III). Asterisks (*) indicate the positive clones that were identified from each PCR screen. A second round of *Cre*-mediated recombination was used to remove the remaining SEPT element from the second allele. Either *LSD1*$^{+/-}$ or *LSD1*$^{-/-}$ clones post *Cre*-LoxP recombination were used in the present study. (**C**) Western blot analysis indicates the loss of LSD1 protein in the nucleus of two independent *LSD1*$^{+/-}$ clones and four *LSD1*$^{-/-}$ clones that were derived from one of the *LSD1*$^{+/-}$ clone. Total H3 was used as a control to normalize for protein loading. qPCR revealed a decrease in *LSD1* mRNA levels due to nonsense-mediated decay following exon 2 disruption. Parental HCT116 cells were used as a control. The *LSD1* mRNA levels were normalized to *GAPDH* (glyceraldehyde-3-phosphate dehydrogenase). Results are means ± S.E.M. ($n = 3$).

CoREST may be due to the different cell types used in the present study.

In addition to its histone substrates, LSD1 has been reported to demethylate Lys^{370} of p53 and repress p53-mediated transcription, as well as its apoptosis-promoting action [18,26]. Additionally, the maintenance DNA methyltransferase DNMT1 has been implicated as another non-histone substrate. It has been reported that methylation of DNMT1 by SET7/9 increases protein turnover and, therefore, the loss of LSD1 demethylase activity was suggested to directly result in reduced levels of DNMT1 and global DNA methylation [13]. These observations prompted us to determine whether the loss of LSD1 affects the levels of either p53 or DNMT1 in HCT116 cells. The loss of LSD1 did not result in significant changes in the basal expression of either the p53 or DNMT1 protein (Figure 2C), clearly indicating that LSD1 is not an absolute requirement for the stabilization of either p53 or DNMT1, as has been suggested previously [13,26].

Since there were no obvious changes in the steady-state levels of either p53 or DNMT1 protein, we sought to determine if the activity of either protein could be affected in the *LSD1*-null cells. To test whether the DNA damage response of p53 was altered, parental HCT116, *LSD1*$^{+/-}$ and *LSD1*$^{-/-}$ cells were exposed to the DNA-damaging agent doxorubicin for 8 and 24 h, after which time the protein levels of p53 and its downstream target p21 were determined by Western blot analysis (Figures 3A and 3B). For each cell line, endogenous p53 protein was activated upon treatment with doxorubicin (Figure 3A) and led to increased p21 transcript and protein levels (Figures 3A–3C). These results indicated that the loss of LSD1 did not affect the function of p53 induced by the DNA damage response with respect to p21

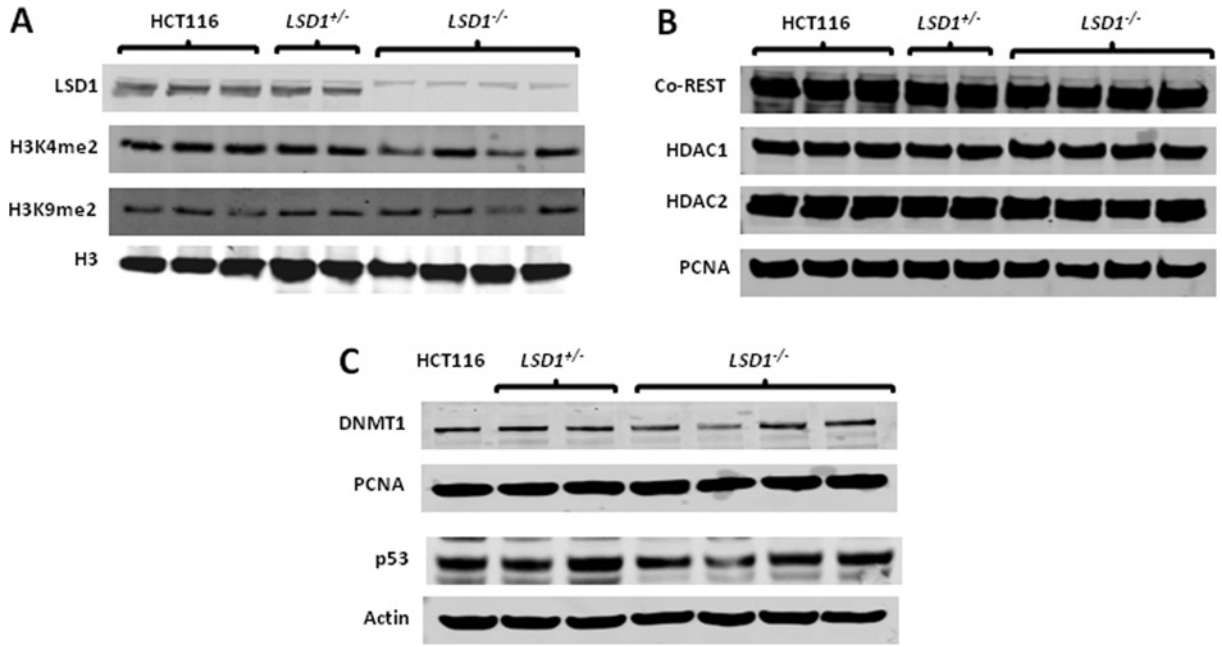

Figure 2 Loss of LSD1 does not result in changes in global level of histone marks, binding partner proteins or non-histone protein substrates

Nuclear extracts (30 μg) from *LSD1*$^{-/-}$, *LSD1*$^{+/-}$ and parental HCT116 cells were loaded in each lane and the methylation status of histone marks (**A**) and the global level of LSD1 binding partner proteins CoREST, HDAC1, HDAC2 (**B**) and DNMT1 (**C**) were determined by Western blot analysis. Total H3 or PCNA were used as loading controls for histone marks or LSD1 nuclear-binding proteins respectively. Whole-cell lysates were extracted from *LSD1*$^{-/-}$, *LSD1*$^{+/-}$ and parental HCT116 cells, and Western blotting using 50 μg of whole-cell lysate from each cell line was performed to detect the protein expression level of p53 (**C**). Actin was used as a loading control.

transcription or protein levels. Interestingly, the basal level of p21 in *LSD1*-null cells was elevated compared with the parental HCT116 or *LSD1*$^{+/-}$ cells (Figures 3A–3C). This elevated p21 level was consistent with the reduction in cell proliferation and the increased population of cells in the G_1-phase of the cell cycle that was observed in the *LSD1*-null cells, as discussed below. These results suggest that LSD1 may have a role in the regulation of cell proliferation via repression of p21, presumably in a p53-independent manner.

To assess whether the promoter of *p21* is directly regulated by LSD1, which consequently would lead to an enrichment of activating histone marks, ChIP analysis was performed using anti-LSD1, anti-H3K4me1/me2/me3 and anti-H3K9ac antibodies in parental HCT116, *LSD1*$^{+/-}$ and *LSD1*$^{-/-}$ cells. The results confirmed that LSD1 is present at the proximal promoter of *p21* in wild-type HCT116 cells (Supplementary Figure S2 at http://www.biochemj.org/bj/449/bj4490459add.htm). However, the transcriptional activating marks H3K4me1/me2/me3 or H3K9ac were not altered in the proximal promoter of *p21* in *LSD1*-null cells. These results indicate that the up-regulation of p21 in *LSD1*-null cells was not directly mediated by changes in the histone targets of LSD1. Therefore it is possible that the increase of p21 in *LSD1*-null cells is an indirect response to the loss of *LSD1*.

To determine if the loss of LSD1 affects genome-wide DNA methylation, even in the absence of changes in steady-state DNMT1 protein levels, COBRA analysis was used to examine the methylation of LINE-1 repeat elements. This strategy has been successfully used as a reliable indicator of whole-genome methylation [34]. The COBRA analysis revealed that the loss of LSD1 did not affect levels of global methylation and, therefore, LSD1 is not an absolute requirement for the stabilization of DNMT1 or its activity (Figure 3D).

On the basis of the observation that neither the global levels of the major histone targets nor the proposed non-histone targets were changed with the loss of LSD1, the possibility that known players in maintaining histone methylation status were compensating for the loss of LSD1 was examined. Lysine methylation is controlled *in vivo* by the opposing activities of lysine methyltransferases and lysine demethylases. Two classes of lysine demethylases have been identified: the FAD-dependent amine oxidases, of which two representatives are known to exist (LSD1 and LSD2), and the Jumonji C domain-containing proteins. LSD2, a homologue of LSD1, is an H3K4me1/me2 demethylase that specifically regulates histone H3K4 methylation within intragenic regions of its target genes [3]. JARID1A and JARID1B are members of the Jumonji C family of demethylases that specifically demethylate H3K4me1/me2/me3 marks that are associated with active genes [5]. SET7/9 is a human histone methyltransferase that can target H3K4 and regulate gene expression [38]. It can also methylate non-histone protein substrates and regulate their transcriptional activity [13,39]. Since the global expression levels of H3K4me2, p53 and DNMT1 were not observed to change in *LSD1*$^{-/-}$ cells (Figures 2A and 2C), we hypothesized that the increase of other histone lysine demethylases, such as LSD2, JARID1A and JARID1B, or a decrease of the histone methyltransferase SET7/9 might compensate for the loss of LSD1. To determine whether there were changes in any of these proteins resulting from the loss of LSD1, the nuclear protein expression levels of LSD2, JARID1A, JARID1B and SET7/9 were analysed in *LSD1*$^{-/-}$ cells. No significant changes in any of the proteins that would be the most obvious players to compensate for the loss of LSD1 were observed (Figure 4). These results suggest the possible existence of another lysine demethylase capable of demethylating the histone and, potentially, non-histone substrates.

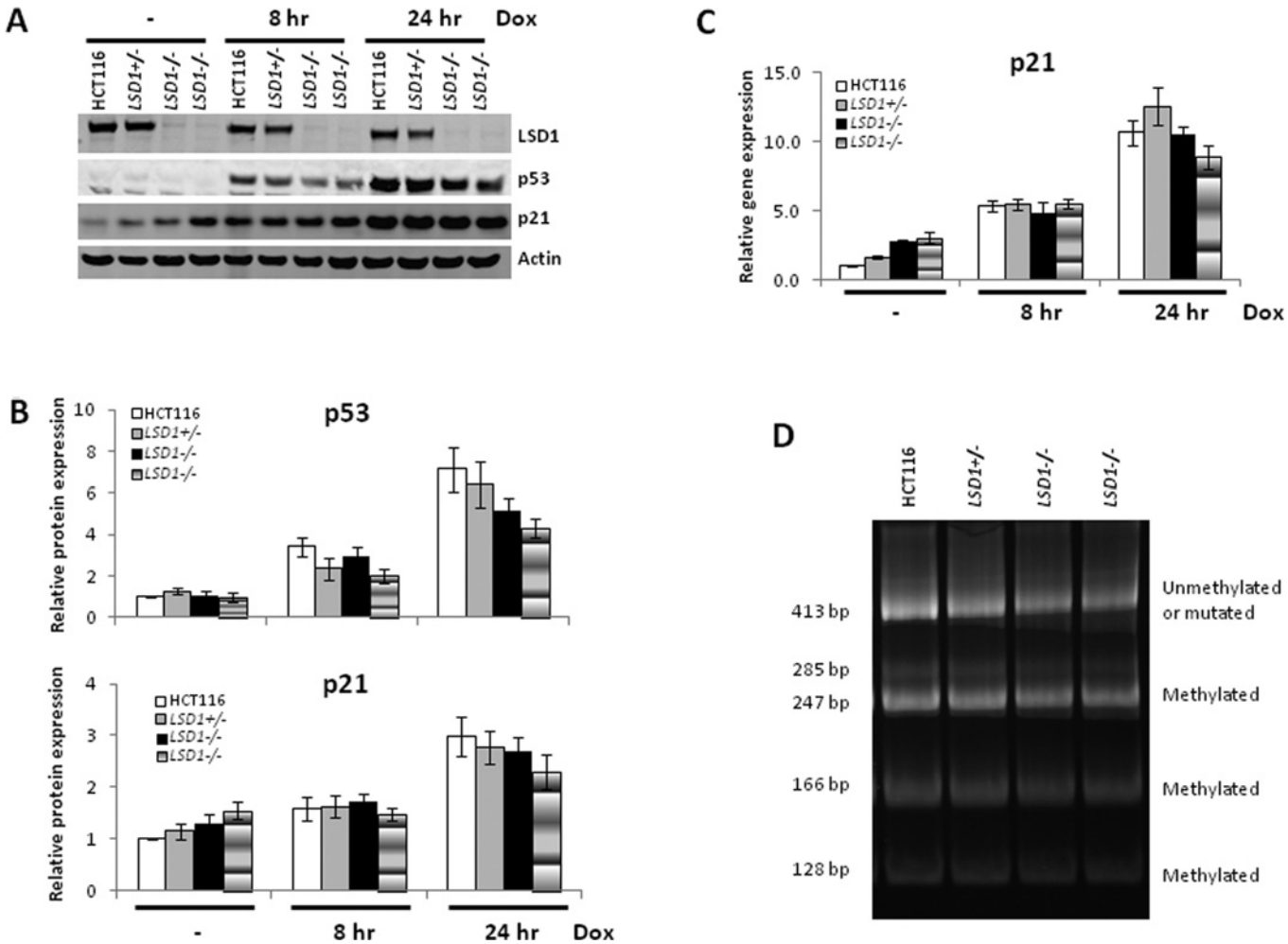

Figure 3 Loss of LSD1 does not affect the stabilization or activity of p53 or DNMT1

(**A**) A DNA-damaging agent induces p53 and p21 expression regardless of LSD1 status. Parental HCT116, *LSD1*$^{+/-}$ and *LSD1*$^{-/-}$ cells were exposed to 1 μM of doxorubicin (Dox) for the indicated times, followed by total protein extraction and Western blot analysis. Actin was used as a loading control. (**B**) Histograms represent the mean protein expression levels of p53 and p21 relative to actin $\pm$ S.E.M., as determined by quantitative immunoblotting using infrared detection and analysis. (**C**) Expression of *p21* mRNA is increased after DNA-damaging agent treatment. qPCR was used to assess the relative mRNA levels of *p21* in parental HCT116, *LSD1*$^{+/-}$ and *LSD1*$^{-/-}$ cells treated as in (**A**). (**D**) Global maintenance methylation (DNMT1 activity) does not change after loss of LSD1. Methylation analysis of the LINE-1 promoter was performed using the COBRA assay. Genomic DNA was isolated from parental HCT116, *LSD1*$^{+/-}$ and *LSD1*$^{-/-}$ cells, treated with sodium bisulfite and non-specific PCR was performed to amplify LINE-1 repetitive elements. The PCR products were then digested with HinfI, which only cuts repetitive elements that were originally methylated. The 285, 247, 166 and 128 bp fragments represent methylated repetitive elements and were not affected by the loss of LSD1. The digested products were separated by polyacrylamide gel electrophoresis and stained with ethidium bromide.

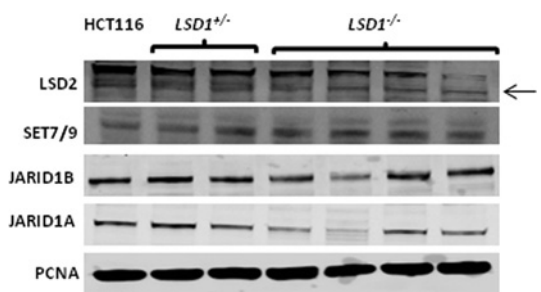

Figure 4 Loss of LSD1 does not change global levels of the histone lysine demethylases LSD2, JARID1A and JARID1B, or the histone methyltrasferase SET7/9

Nuclear extracts from *LSD1*$^{-/-}$, *LSD1*$^{+/-}$ and parental HCT116 cells were analysed by Western blotting using 30 μg of nuclear extract from each cell line. PCNA was used as a loading control. The arrow indicates the correct size of LSD2.

The loss of LSD1 significantly reduces cell proliferation

LSD1 has the ability to broadly repress gene expression by removing the transcriptional activating mark H3K4me2 [15,18–20,23,38–40]. It has also been implicated in maintaining the malignant phenotype by down-regulating tumour-suppressor gene expression and up-regulating the oncogenic phenotype [25,27–31,41]. Therefore we hypothesized that the loss of LSD1 would lead to a reduced growth rate in the colorectal cancer cells lacking LSD1. To this end, a 4-day growth curve of *LSD1*$^{-/-}$, *LSD1*$^{+/-}$ and parental HCT116 cells was performed and indicated that there was a significant growth delay starting on day 2 in the *LSD1*$^{-/-}$ cells compared with the *LSD1*$^{+/-}$ and parental cells (Figure 5A). This decrease in growth rate was accompanied by significant decreases in S- and G_2/M-phase cells in the *LSD1*-null cells, with a concomitant increase in G_1-phase cells (Figure 5B). However, there was no indication that the decrease in the growth rate was accompanied by an increase in apoptosis, as there was no change

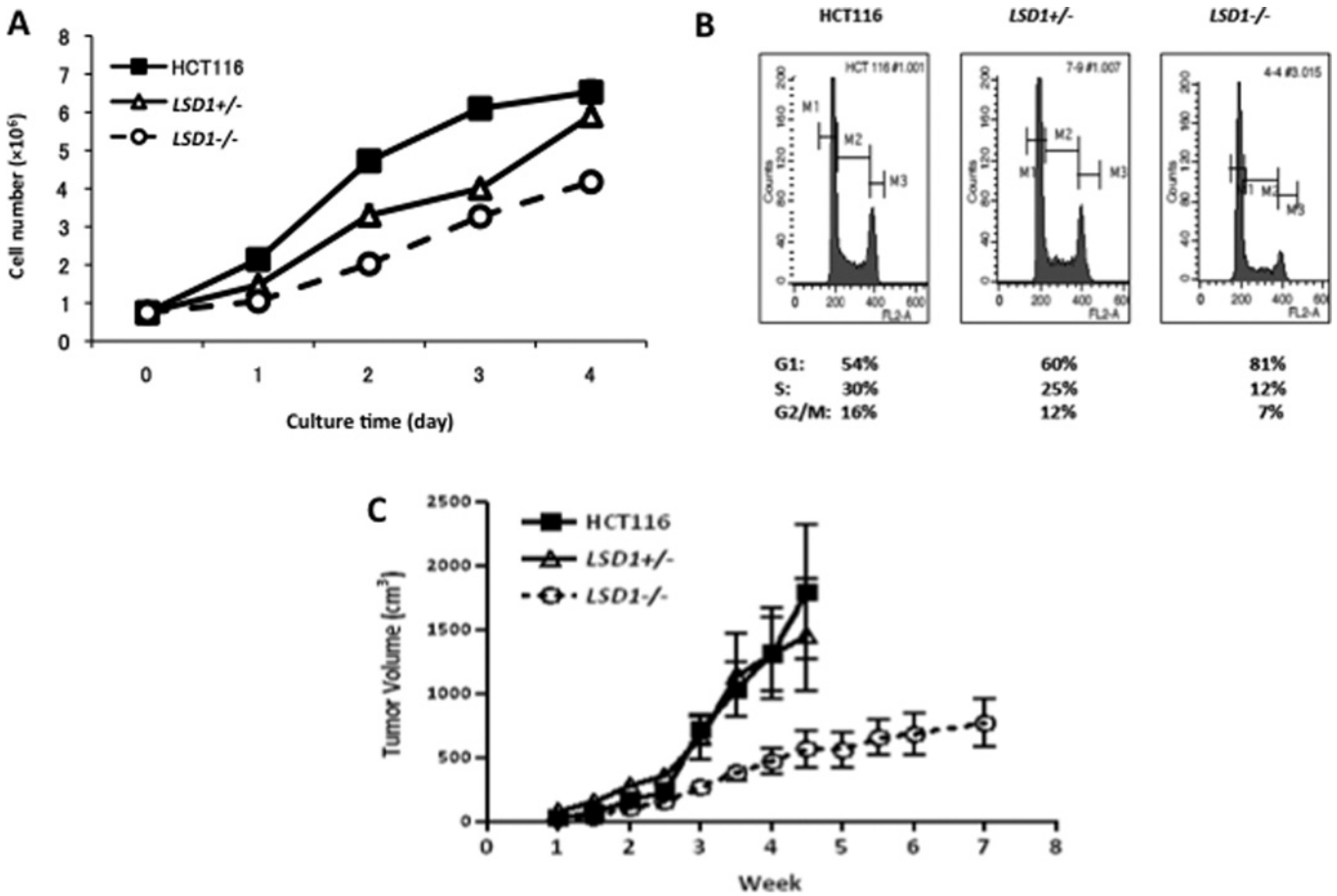

Figure 5 Loss of LSD1 significantly reduces cell proliferation both *in vitro* and *in vivo*

(**A**) The growth rate of $LSD1^{-/-}$ cells was compared with $LSD1^{+/-}$ or parental HCT116 cells by counting cells over a 4-day period following an initial plating density of 7.5×10^5 cells per T-25 flask. (**B**) Cell-cycle analyses of $LSD1^{-/-}$, $LSD1^{+/-}$ and parental HCT116 cells were performed by propidium iodide staining and FACS analyses. The percentages of cells with G_1- (M_1), S- (M_2) or G_2/M- (M_3) DNA content are as indicated. (**C**) Subcutaneous tumours were generated by injecting 1.0×10^7 cells into the flanks of nude mice. The measurement of tumours began 10 days after implantation and continued twice weekly for 7 weeks. Results are mean tumour volumes $\pm$ S.E.M. ($n=5$).

in the sub-G_1 (apoptotic) cell population (Figure 5B). These results suggest that the loss of LSD1 expression leads to a partial restoration of tumour cell growth control that is concurrent with an up-regulation of the basal level of p21 expression (Figures 3A–3C) and not a result of increased apoptosis.

To determine whether the decrease in growth rate was simply an artefact of the *in vitro* conditions, we expanded our growth studies to an *in vivo* mouse model. Parental HCT116, $LSD1^{+/-}$ and $LSD1^{-/-}$ cells were implanted subcutaneously in BALB/$c^{nu/nu}$ mice and their growth was followed for up to 7 weeks. Each genotype produced detectable tumours within 1–2 weeks after injection; however, the $LSD1^{-/-}$ cell tumours grew at a significantly slower rate than the tumours of $LSD1^{+/-}$ or parental HCT116 cells (Figure 5C). Taken together, our *in vitro* and *in vivo* studies strongly suggest that LSD1 plays a critical role in the regulation of cell proliferation. Further, this decreased growth rate is consistent with previous *in vivo* studies showing a decrease in tumour growth rate when animals were treated with inhibitors of LSD1 [42], indicating that LSD1 is an important player in determining tumour growth rate.

Defining LSD1 target genes

Although global levels of H3K4 methylation were not altered in the *LSD1*-null cells, the growth studies clearly indicate that the loss of LSD1 significantly affects growth, suggesting that the loss of LSD1 alters gene expression profiles. Because LSD1 is a component of multiple transcriptional repressor complexes and thus has the ability to broadly repress transcription, we sought to determine the genes or gene families whose expression is directly or indirectly affected by LSD1. Therefore total RNA was isolated from $LSD1^{-/-}$, $LSD1^{+/-}$ and parental HCT116 cells and used to perform a comparative microarray analysis using the Illumina HumanHT-12 v4 Expression BeadChip platform, which covers more than 47000 probes derived from the NCBI Reference Sequence database. Microarray data were normalized by robust spline normalization after variance-stabilizing transformation. With a P value-detection threshold of 0.01, probes with a detection call greater than 0 were selected and then filtered with a coefficient of variation greater than 0.1. Finally, a total of 84 probes that correspond to 72 genes were identified and a heat map was generated to compare the expression profiles between $LSD1^{-/-}$, $LSD1^{+/-}$ and parental HCT116 cells (Figure 6A). Although there was considerable similarity between the parental HCT116 cells and the $LSD1^{+/-}$ cells with respect to the gene expression profiles, significantly different expression patterns were observed in the 72 genes between the $LSD1^{-/-}$ cells and either the $LSD1^{+/-}$ or parental HCT116 cells. Interestingly, most of genes identified were functionally related to the immune response. An analysis of the functionally related gene groups among our up- or

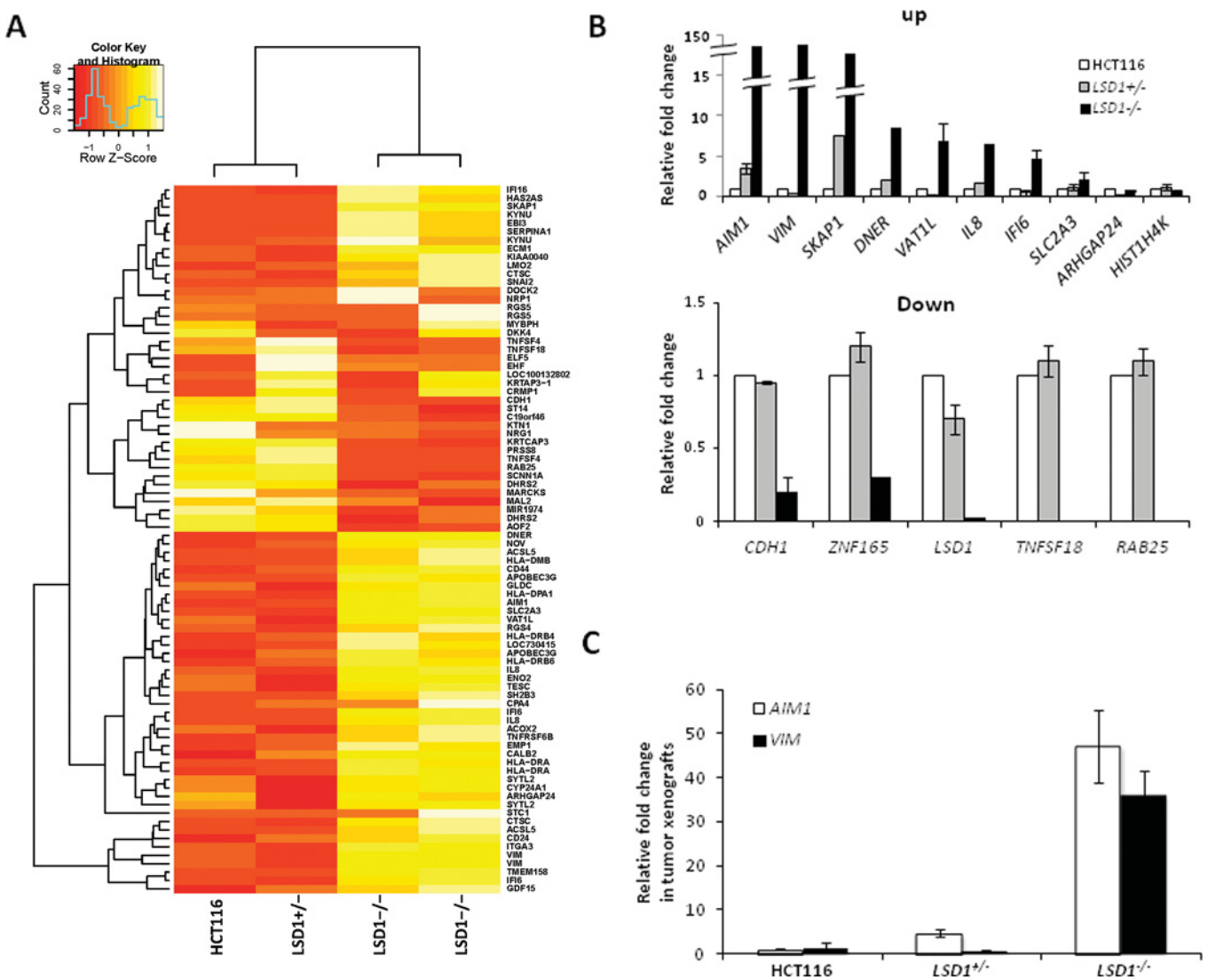

Figure 6 Loss of LSD1 leads to changes in gene expression

(**A**) A heat map was generated to compare gene expression patterns between the three genotypes. Columns represent the samples and rows represent the probes. The key in the upper left-hand corner shows the relative differential expression corresponding to the colours in the heat map. (**B**) qPCR validation on genes up- and down-regulated in *LSD1*$^{-/-}$ cells. Values are expressed relative to the level of gene expression in parental HCT116 cells and normalized against GAPDH. Results are means ± S.E.M. ($n = 3$). (**C**) qPCR validation of *AIM1* (absent in melanoma 1) and *VIM* expression in xenograft tumours. Values are expressed relative to the level of gene expression in tumour xenografts of parental HCT116 cells and normalized against GAPDH.

down-regulated LSD1 target gene list was performed using the DAVID (database for annotation, visualization and integrated discovery) and confirmed an enrichment in the expression of the genes involved in the immune response.

To further verify the microarray results, the expression levels of ten up-regulated and five down-regulated genes were quantified by qPCR (Figure 6B). With the sole exception of *HIST1H4K* (histone cluster 1, H4k), the qPCR results were concordant with the microarray analyses. *ARHGAP24* (Rho GTPase activating protein 24) showed an increase in expression in the *LSD1*$^{-/-}$ cells relative to the *LSD1*$^{+/-}$, but not the parental HCT116 cells. We then chose two of the most up-regulated genes, *AIM1* (absent in melanoma 1) and *VIM* (vimentin), for further validation of expression in mouse tumour xenografts. Both genes demonstrated significant increases in the tumours generated by the *LSD1*$^{-/-}$ cells relative to the *LSD1*$^{+/-}$ or parental HCT116 cells (Figure 6C). These data indicate a correlation between LSD1 loss and increased LSD1 target gene expression both *in vitro* and *in vivo*.

In order to verify that the up-regulation of these genes was a result of being a direct target of LSD1, ChIP was performed to test the occupancy of LSD1 at the target promoters in parental HCT116 cells. We chose four genes, *VIM*, *VAT1L* (vesicle amine transport protein 1 homologue-like), *IFI6* (interferon α-inducible protein 6) and *IL8* (interleukin 8), mapped LSD1 localization at several sites in their promoters, and observed higher levels of LSD1 occupancy at sites near the TSSs (transcription start sites) than at more distal 5′-regions (approximately 3000 bp upstream of TSS) (Figure 7A). Furthermore, in the absence of LSD1, we detected increases in the levels of H3K4me2/me3 and H3K9ac around the TSS of the *VAT1L* gene (Figure 7B), indicative of the loss of LSD1 enzymatic activity and increased transcription. These data indicate that the loss of LSD1 at the promoters of specific genes greatly influences the abundance of activating histone marks with concomitant increases in the expression of target genes.

The results of the present study are surprising in that the loss of LSD1 did not alter the global levels of H3K4 methylation or

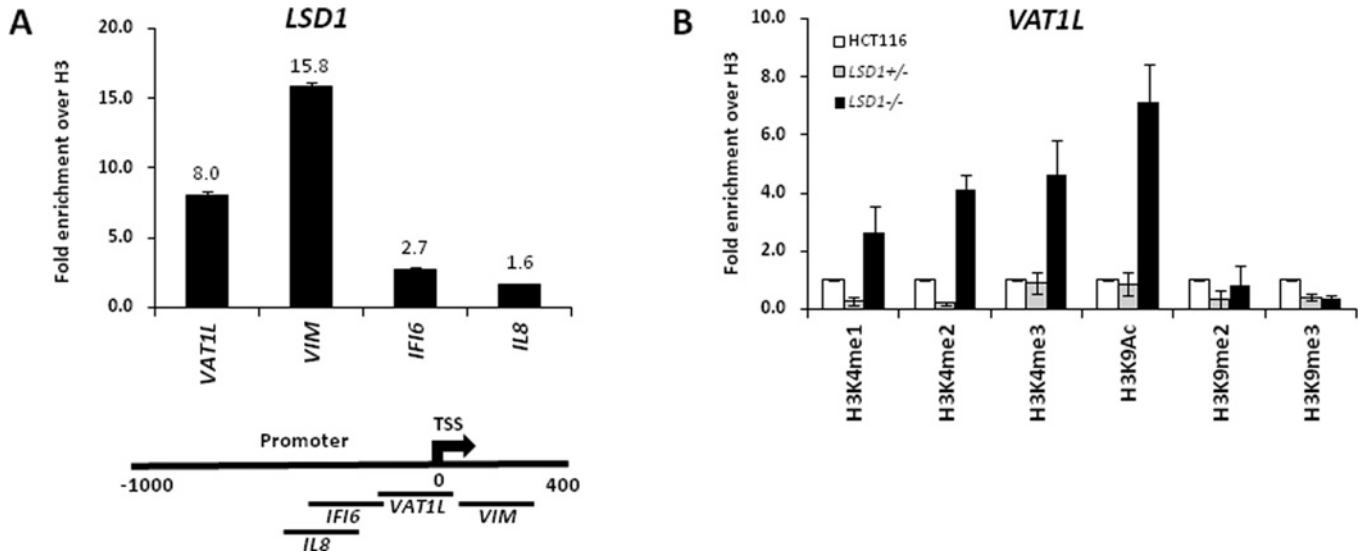

Figure 7 Loss of LSD1 at the promoters of specific genes increases the levels of active histone marks with concomitant increased expression of target genes

(**A**) Quantitative ChIP analysis was used to determine the occupancy of LSD1 at the promoters of *VAT1L, VIM, IFI6* (interferon α-inducible protein 6) and *IL8* (interleukin 8) in parental HCT116 cells. The schematic indicates the relative positions of primers used for quantitative ChIP. The relative enrichment of LSD1 levels for the distal promoter region of each gene (approximately -3000 bp from the TSS) was set to a value of 1. (**B**) The composite graph indicates the enrichment of histone marks at the indicated region of the *VAT1L* promoter. The relative enrichment of histone marks for parental HCT116 cells was set to a value of 1. Results are means $\pm$ S.E.M. for three independent immunoprecipitations with PCR performed in triplicate.

change the stability or the activity of two proposed non-histone protein targets of LSD1, p53 and DNMT1. It is possible that the differences observed are a result of previous studies conducted in transient knockdown systems compared with this long-term knockout system. It is clear, however, that the loss of LSD1 does have a profound effect on gene expression, and at least some of those changes are concurrent with local increases in the enzymatic target of LSD1, the H3K4me2 transcriptional activating mark. These results suggest two possibilities: (i) the existence of an unidentified histone demethylase that compensates for the loss of LSD1 in both histone and non-histone protein demethylation and/or (ii) DNMT1 and p53 are not actual substrates of LSD1.

Finally, the high expression of LSD1 in several types of cancer, coupled with the known roles of this enzyme in transcriptional repression, has heightened interest in LSD1 as a potential therapeutic target for cancer [39,40,43–45]. *In vitro* results using LSD1 inhibitors in the treatment of cancer cells have resulted in increases in methylated H3K4 with increased expression of various previously silenced tumour-suppressor genes [38,42]. The *in vivo* treatment of established human colon tumours in nude mice with inhibitors of LSD1 resulted in a dramatic decrease in tumour size, and the use of LSD1 inhibitors in combination with a DNMT1 inhibitor demonstrated a synergistic reactivation of specific aberrantly silenced genes with a concurrent synergistic growth inhibition of the established xenografts [42]. Additionally, LSD1 inhibitors have been demonstrated to reactivate differentiation pathways in ATRA (all-*trans* retinoic acid)-resistant human leukaemia cells when used in combination with ATRA [42]. These data firmly establish LSD1 as a target for chemotherapy and demonstrate that inhibitors of this enzyme have considerable promise, both when used alone and in combination with other agents. Importantly, the *LSD1*$^{-/-}$ model described in the present study will provide an excellent platform, which should allow the definition of the specific roles of LSD1 in tumour formation, aid in the discovery of new LSD1 inhibitors, and define the on-target and off-target effects of potential LSD1 inhibitors.

AUTHOR CONTRIBUTION

Lihua Jin, Christin Hanigan, Yu Wu, Ben Ho Park, Patrick Woster and Robert Casero Jr designed the experiments. Lihua Jin, Christin Hanigan, Yu Wu and Wei Wang performed the experiments, and Lihua Jin, Christin Hanigan, Yu Wu, Wei Wang, Ben Ho Park, Patrick Woster and Robert Casero Jr analysed the data and wrote the paper.

ACKNOWLEDGEMENT

We thank Tracy Murray Stewart for her careful review of the paper prior to submission.

FUNDING

This work was funded, in part, by the National Institutes of Health [grant numbers CA51085, CA58184, CA98454 and CA149095] and the Samuel Waxman Cancer Research Foundation.

REFERENCES

1 Jenuwein, T. and Allis, C. D. (2001) Translating the histone code. Science **293**, 1074–1080
2 Shi, Y., Lan, F., Matson, C., Mulligan, P., Whetstine, J. R., Cole, P. A., Casero, R. A. and Shi, Y. (2004) Histone demethylation mediated by the nuclear amine oxidase homolog LSD1. Cell **119**, 941–953
3 Fang, R., Barbera, A. J., Xu, Y., Rutenberg, M., Leonor, T., Bi, Q., Lan, F., Mei, P., Yuan, G. C., Lian, C. et al. (2010) Human LSD2/KDM1b/AOF1 regulates gene transcription by modulating intragenic H3K4me2 methylation. Mol. Cell **39**, 222–233
4 Ciccone, D. N., Su, H., Hevi, S., Gay, F., Lei, H., Bajko, J., Xu, G., Li, E. and Chen, T. (2009) KDM1B is a histone H3K4 demethylase required to establish maternal genomic imprints. Nature **461**, 415–418
5 Shi, Y. and Whetstine, J. R. (2007) Dynamic regulation of histone lysine methylation by demethylases. Mol. Cell **25**, 1–14
6 Chen, Y., Yang, Y., Wang, F., Wan, K., Yamane, K., Zhang, Y. and Lei, M. (2006) Crystal structure of human histone lysine-specific demethylase 1 (LSD1). Proc. Natl. Acad. Sci. U.S.A. **103**, 13956–13961
7 Tochio, N., Umehara, T., Koshiba, S., Inoue, M., Yabuki, T., Aoki, M., Seki, E., Watanabe, S., Tomo, Y., Hanada, M. et al. (2006) Solution structure of the SWIRM domain of human histone demethylase LSD1. Structure **14**, 457–468
8 Stavropoulos, P., Blobel, G. and Hoelz, A. (2006) Crystal structure and mechanism of human lysine-specific demethylase-1. Nat Struct. Mol. Biol. **13**, 626–632

9 Wang, Y., Devereux, W., Woster, P. M., Stewart, T. M., Hacker, A. and Casero, Jr, R. A. (2001) Cloning and characterization of a human polyamine oxidase that is inducible by polyamine analogue exposure. Cancer Res. **61**, 5370–5373

10 Yang, M., Gocke, C. B., Luo, X., Borek, D., Tomchick, D. R., Machius, M., Otwinowski, Z. and Yu, H. (2006) Structural basis for CoREST-dependent demethylation of nucleosomes by the human LSD1 histone demethylase. Mol. Cell. **23**, 377–387

11 Forneris, F., Binda, C., Adamo, A., Battaglioli, E. and Mattevi, A. (2007) Structural basis of LSD1–CoREST selectivity in histone H3 recognition. J. Biol. Chem. **282**, 20070–20074

12 Anand, R. and Marmorstein, R. (2007) Structure and mechanism of lysine-specific demethylase enzymes. J. Biol. Chem. **282**, 35425–35429

13 Wang, J., Hevi, S., Kurash, J. K., Lei, H., Gay, F., Bajko, J., Su, H., Sun, W., Chang, H., Xu, G. et al. (2009) The lysine demethylase LSD1 (KDM1) is required for maintenance of global DNA methylation. Nat. Genet. **41**, 125–129

14 Wang, J., Scully, K., Zhu, X., Cai, L., Zhang, J., Prefontaine, G. G., Krones, A., Ohgi, K. A., Zhu, P., Garcia-Bassets, I. et al. (2007) Opposing LSD1 complexes function in developmental gene activation and repression programmes. Nature **446**, 882–887

15 Foster, C. T., Dovey, O. M., Lezina, L., Luo, J. L., Gant, T. W., Barlev, N., Bradley, A. and Cowley, S. M. (2010) Lysine-specific demethylase 1 regulates the embryonic transcriptome and CoREST stability. Mol. Cell. Biol. **30**, 4851–4863

16 Sun, G., Alzayady, K., Stewart, R., Ye, P., Yang, S., Li, W. and Shi, Y. (2010) Histone demethylase LSD1 regulates neural stem cell proliferation. Mol. Cell. Biol. **30**, 1997–2005

17 Su, S. T., Ying, H. Y., Chiu, Y. K., Lin, F. R., Chen, M. Y. and Lin, K. I. (2009) Involvement of histone demethylase LSD1 in Blimp-1-mediated gene repression during plasma cell differentiation. Mol. Cell. Biol. **29**, 1421–1431

18 Scoumanne, A. and Chen, X. (2007) The lysine-specific demethylase 1 is required for cell proliferation in both p53-dependent and -independent manners. J. Biol. Chem. **282**, 15471–15475

19 Janzer, A., Lim, S., Fronhoffs, F., Niazy, N., Buettner, R. and Kirfel, J. (2012) Lysine-specific demethylase 1 (LSD1) and histone deacetylase 1 (HDAC1) synergistically repress proinflammatory cytokines and classical complement pathway components. Biochem. Biophys. Res. Comm. **421**, 665–670

20 Li, Y., Deng, C., Hu, X., Patel, B., Fu, X., Qiu, Y., Brand, M., Zhao, K. and Huang, S. (2012) Dynamic interaction between TAL1 oncoprotein and LSD1 regulates TAL1 function in hematopoiesis and leukemogenesis. Oncogene, doi:10.1038/onc.2012.8.

21 Musri, M. M., Carmona, M. C., Hanzu, F. A., Kaliman, P., Gomis, R. and Parrizas, M. (2010) Histone demethylase LSD1 regulates adipogenesis. J. Biol. Chem. **285**, 30034–30041

22 Whyte, W. A., Bilodeau, S., Orlando, D. A., Hoke, H. A., Frampton, G. M., Foster, C. T., Cowley, S. M. and Young, R. A. (2012) Enhancer decommissioning by LSD1 during embryonic stem cell differentiation. Nature **482**, 221–225

23 Metzger, E., Wissmann, M., Yin, N., Muller, J. M., Schneider, R., Peters, A. H., Gunther, T., Buettner, R. and Schule, R. (2005) LSD1 demethylates repressive histone marks to promote androgen-receptor-dependent transcription. Nature **437**, 436–439

24 Wissmann, M., Yin, N., Muller, J. M., Greschik, H., Fodor, B. D., Jenuwein, T., Vogler, C., Schneider, R., Gunther, T., Buettner, R. et al. (2007) Cooperative demethylation by JMJD2C and LSD1 promotes androgen receptor-dependent gene expression. Nat. Cell Biol. **9**, 347–353

25 Lim, S., Janzer, A., Becker, A., Zimmer, A., Schule, R., Buettner, R. and Kirfel, J. (2010) Lysine-specific demethylase 1 (LSD1) is highly expressed in ER-negative breast cancers and a biomarker predicting aggressive biology. Carcinogenesis **31**, 512–520

26 Huang, J., Sengupta, R., Espejo, A. B., Lee, M. G., Dorsey, J. A., Richter, M., Opravil, S., Shiekhattar, R., Bedford, M. T., Jenuwein, T. and Berger, S. L. (2007) p53 is regulated by the lysine demethylase LSD1. Nature **449**, 105–108

27 Schulte, J. H., Lim, S., Schramm, A., Friedrichs, N., Koster, J., Versteeg, R., Ora, I., Pajtler, K., Klein-Hitpass, L., Kuhfittig-Kulle, S. et al. (2009) Lysine-specific demethylase 1 is strongly expressed in poorly differentiated neuroblastoma: implications for therapy. Cancer Res. **69**, 2065–2071

28 Hayami, S., Kelly, J. D., Cho, H. S., Yoshimatsu, M., Unoki, M., Tsunoda, T., Field, H. I., Neal, D. E., Yamaue, H., Ponder, B. A. et al. (2011) Overexpression of LSD1 contributes to human carcinogenesis through chromatin regulation in various cancers. Int. J. Cancer **128**, 574–586

29 Kahl, P., Gullotti, L., Heukamp, L. C., Wolf, S., Friedrichs, N., Vorreuther, R., Solleder, G., Bastian, P. J., Ellinger, J., Metzger, E. et al. (2006) Androgen receptor coactivators lysine-specific histone demethylase 1 and four and a half LIM domain protein 2 predict risk of prostate cancer recurrence. Cancer Res. **66**, 11341–11347

30 Lv, T., Yuan, D., Miao, X., Lv, Y., Zhan, P., Shen, X. and Song, Y. (2012) Over-expression of LSD1 promotes proliferation, migration and invasion in non-small cell lung cancer. PloS ONE **7**, e35065

31 Schildhaus, H. U., Riegel, R., Hartmann, W., Steiner, S., Wardelmann, E., Merkelbach-Bruse, S., Tanaka, S., Sonobe, H., Schule, R., Buettner, R. and Kirfel, J. (2011) Lysine-specific demethylase 1 is highly expressed in solitary fibrous tumors, synovial sarcomas, rhabdomyosarcomas, desmoplastic small round cell tumors, and malignant peripheral nerve sheath tumors. Hum. Pathol. **42**, 1667–1675

32 Rago, C., Vogelstein, B. and Bunz, F. (2007) Genetic knockouts and knockins in human somatic cells. Nat. Protocols **2**, 2734–2746

33 Konishi, H., Lauring, J., Garay, J. P., Karakas, B., Abukhdeir, A. M., Gustin, J. P., Konishi, Y. and Park, B. H. (2007) A PCR-based high-throughput screen with multiround sample pooling: application to somatic cell gene targeting. Nat. Protocol. **2**, 2865–2874

34 Yang, A. S., Estecio, M. R., Doshi, K., Kondo, Y., Tajara, E. H. and Issa, J. P. (2004) A simple method for estimating global DNA methylation using bisulfite PCR of repetitive DNA elements. Nucleic Acids Res. **32**, e38

35 Du, P., Kibbe, W. A. and Lin, S. M. (2008) lumi: a pipeline for processing Illumina microarray. Bioinformatics **24**, 1547–1548

36 Lin, S. M., Du, P., Huber, W. and Kibbe, W. A. (2008) Model-based variance-stabilizing transformation for Illumina microarray data. Nucleic Acids Res. **36**, e11

37 McGarvey, K. M., Fahrner, J. A., Greene, E., Martens, J., Jenuwein, T. and Baylin, S. B. (2006) Silenced tumor suppressor genes reactivated by DNA demethylation do not return to a fully euchromatic chromatin state. Cancer Res. **66**, 3541–3549

38 Huang, Y., Greene, E., Murray Stewart, T., Goodwin, A. C., Baylin, S. B., Woster, P. M. and Casero, Jr, R. A. (2007) Inhibition of lysine-specific demethylase 1 by polyamine analogues results in reexpression of aberrantly silenced genes. Proc. Natl. Acad. Sci. U.S.A. **104**, 8023–8028

39 Lin, T., Ponn, A., Hu, X., Law, B. K. and Lu, J. (2010) Requirement of the histone demethylase LSD1 in Snai1-mediated transcriptional repression during epithelial–mesenchymal transition. Oncogene **29**, 4896–4904

40 Schenk, T., Chen, W. C., Gollner, S., Howell, L., Jin, L., Hebestreit, K., Klein, H. U., Popescu, A. C., Burnett, A., Mills, K. et al. (2012) Inhibition of the LSD1 (KDM1A) demethylase reactivates the all-*trans*-retinoic acid differentiation pathway in acute myeloid leukemia. Nat. Med. **18**, 605–611

41 Harris, W. J., Huang, X., Lynch, J. T., Spencer, G. J., Hitchin, J. R., Li, Y., Ciceri, F., Blaser, J. G., Greystoke, B. F., Jordan, A. M. et al. (2012) The histone demethylase KDM1A sustains the oncogenic potential of MLL-AF9 leukemia stem cells. Cancer Cell **21**, 473–487

42 Huang, Y., Stewart, T. M., Wu, Y., Baylin, S. B., Marton, L. J., Perkins, B., Jones, R. J., Woster, P. M. and Casero, Jr, R. A. (2009) Novel oligoamine analogues inhibit lysine-specific demethylase 1 and induce reexpression of epigenetically silenced genes. Clin. Cancer Res. **15**, 7217–7228

43 Lokken, A. A. and Zeleznik-Le, N. J. (2012) Breaking the LSD1/KDM1A addiction: therapeutic targeting of the epigenetic modifier in AML. Cancer Cell **21**, 451–453

44 Singh, M. M., Manton, C. A., Bhat, K. P., Tsai, W. W., Aldape, K., Barton, M. C. and Chandra, J. (2011) Inhibition of LSD1 sensitizes glioblastoma cells to histone deacetylase inhibitors. Neuro-oncology **13**, 894–903

45 Wu, C. Y., Hsieh, C. Y., Huang, K. E., Chang, C. and Kang, H. Y. (2011) Cryptotanshinone down-regulates androgen receptor signaling by modulating lysine-specific demethylase 1 function. Int. J. Cancer **131**, 1423–1434

Received 28 August 2012/15 October 2012; accepted 17 October 2012
Published as BJ Immediate Publication 17 October 2012, doi:10.1042/BJ20121360

Biochem. J. (2013) **449**, 459–468 (Printed in Great Britain) doi:10.1042/BJ20121360

SUPPLEMENTARY ONLINE DATA

Loss of LSD1 (lysine-specific demethylase 1) suppresses growth and alters gene expression of human colon cancer cells in a p53- and DNMT1 (DNA methyltransferase 1)-independent manner

Lihua JIN*, Christin L. HANIGAN*, Yu WU*, Wei WANG*†, Ben Ho PARK*, Patrick M. WOSTER‡ and Robert A. CASERO, Jr*[1]

*The Sidney Kimmel Comprehensive Cancer Center at Johns Hopkins, The Johns Hopkins University School of Medicine, Baltimore, MD 21287, U.S.A., †Predoctoral Training Program in Human Genetics, The Johns Hopkins University School of Medicine, Baltimore, MD 21287, U.S.A., and ‡Department of Drug Discovery and Biomedical Sciences, The Medical University of South Carolina, Charleston, SC 29425, U.S.A.

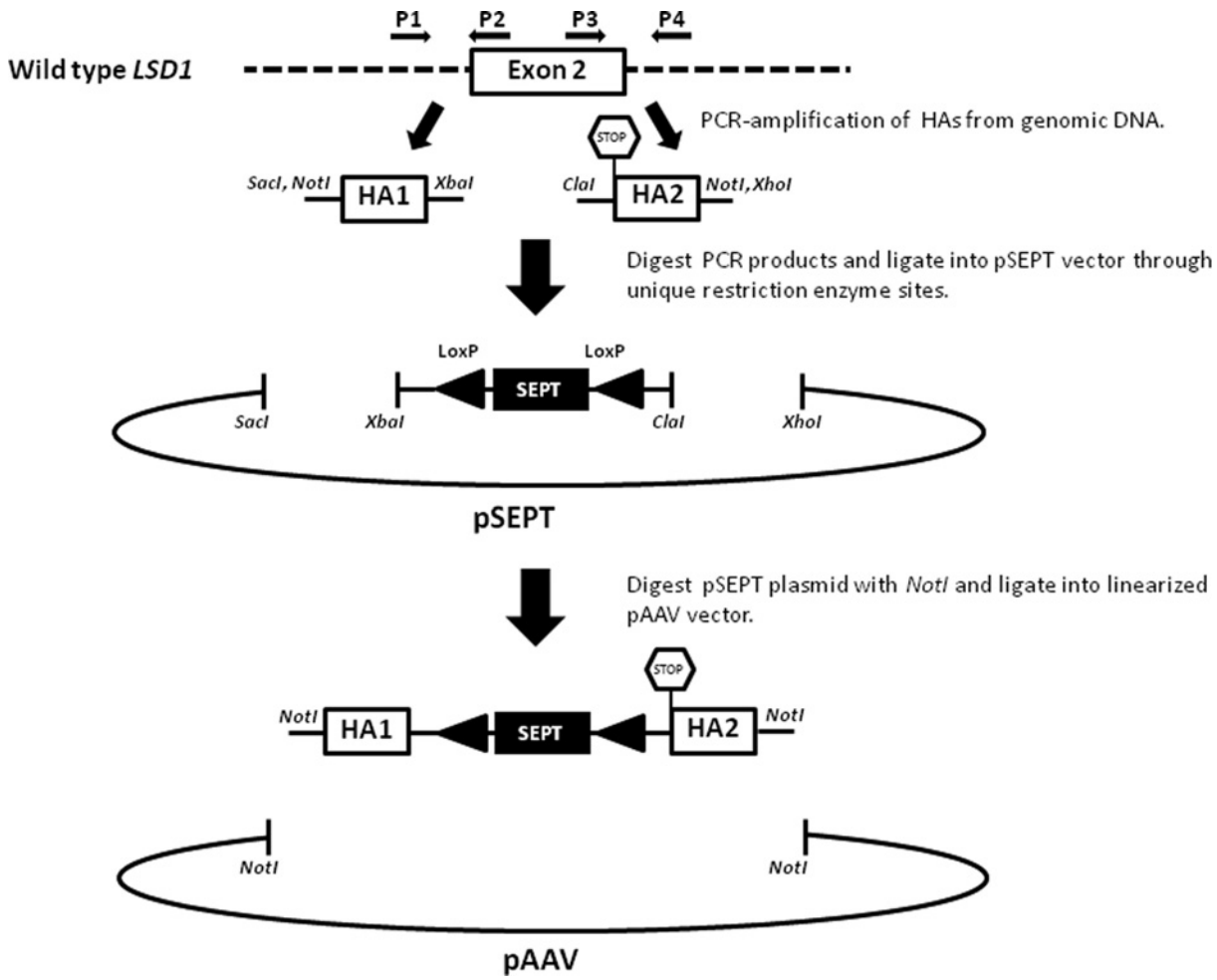

Figure S1 Construction of the pAAV-based targeting vector

HA1 and HA2 were PCR-amplified from HCT116 genomic DNA with primers (P1, P2, P3 and P4) and each contained unique restriction enzyme sites. PCR products were digested and ligated into the pSEPT vector through these restriction enzyme sites. The NotI sites in HA1 and HA2 allowed the cloning of the two HAs, and the SEPT/LoxP cassette into the pAAV vector containing the ITRs (inverted terminal repeats) sequences necessary for viral packaging.

[1] To whom correspondence should be addressed (email rcasero@jhmi.edu).

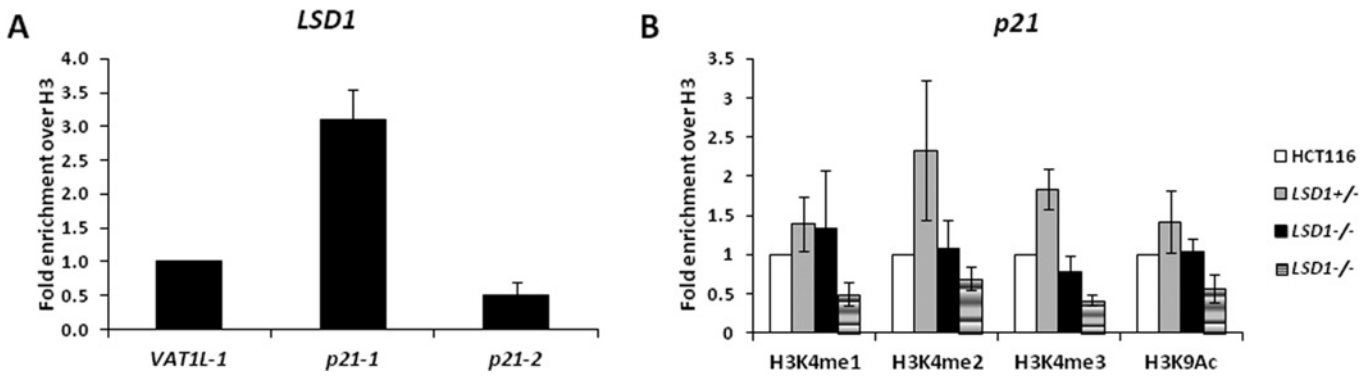

Figure S2 ChIP/qPCR occupancy analysis of the *p21* promoter

(**A**) LSD1 binds the *p21* proximal promoter in the wild-type HCT116 cells. The highest enrichment of LSD1 detected was located 48 bp upstream of the TSS (*p21*-1) as compared with 418 bp upstream of the TSS (*p21*-2). The relative enrichment of LSD1 levels for the distal promoter region of *VAT1L* gene (approximately 5000 bp upstream of the TSS) (*VAT1L*-1) was set to a value of 1. (**B**) Loss of LSD1 at the *p21* promoter does not alter the level of active histone marks. The composite graph shows levels of histone marks at the proximal region of the *p21* promoter (48 bp upstream of the TSS) as normalized to H3, indicating no enrichment of the active marks at *p21* proximal promoter. The relative enrichment of histone modifications for the parental HCT116 cells was set to a value of 1. Results are means $\pm$ S.E.M. for three independent immunoprecipitations with PCR performed in triplicate.

Table S1 Primers used in the present study

AIM1, absent in melanoma 1; ARHGAP24, Rho GTPase activating protein 24; CDH1, cadherin 1, type 1, E-cadherin; DNER, Delta/Notch-like epidermal growth factor repeat-containing; -F, forward; HIST1H4K, histone cluster 1, H4k; IFI6, interferon α-inducible protein 6; IL8, interleukin 8; -R, reverse; SKAP, Src kinase-associated phosphoprotein; SLC2A3, solute carrier family 2 A3; TNFSF18, tumour necrosis factor (ligand) superfamily, member 18; ZNF165, zinc finger protein 165.

Primer	Sequence (5′→3′)	Use
P1	GAAGAGCTCGCGGCCGCTTACCCTCA	Forward primer for HA1. The underlined sequence represents the SacI and NotI sites
P2	GCCTCTAGATTGGCATTTCTC	Reverse primer for HA1. The underlined sequence represents XbaI site
P3	GCCATCGATTAGATAACTGAAAGCAGAGA	Forward primer for HA2. The underlined sequence represents ClaI site
P4	GACCTCGAGGCGGCCGCCTAAAAGAA	Reverse primer for HA2. The underlined sequence represents XhoI and NotI sites
PA	GTGGAAACCATGTTGTCTTTG	Forward primer for screening for the first allele recombination
PB	AAGTCATGCCCGCTTTTG	Reverse primer for screening for the first allele recombination
PC	GGAAACCATGTTGTCTTTGC	Forward primer for screening for the second allele recombination
PD	CATATGCACAGTGGTACCTT	Reverse primer for screening for the second allele recombination
AIM1-F	TGGAGCTTGAAGTCCGATG	Forward primer for qPCR
AIM1-R	CCCACACTTGTGTAAACTTCTC	Reverse primer for qPCR
VIM-F	GCGTGACGTACGTCAGCAATA	Forward primer for qPCR
VIM-R	GCGGCCAATAGTGTCTTGGTA	Reverse primer for qPCR
SKAP1-F	GGGTGACCTCATCCGTATTC	Forward primer for qPCR
SKAP1-R	CCTCATAAAGGCAGGAGAGAG	Reverse primer for qPCR
DNER-F	ACAGCGAGTTCAGCAATG	Forward primer for qPCR
DNER-R	TTTTAATCAGTGTGACCAAGGG	Reverse primer for qPCR
VAT1L-F	ATCAAGCCTGTGGTGGACTC	Forward primer for qPCR
VAT1L-R	TGCTTCACTGGTCTCTGTGC	Reverse primer for qPCR
IL8-F	TGAGAGTGATTGAGAGTGGAC	Forward primer for qPCR
IL8-R	CACTGATTCTTGGATACCACAG	Reverse primer for qPCR
IFI6-F	TGGTCTGCGATCCTGAATG	Forward primer for qPCR
IFI6-R	CTCATCCTCCTCACTATCGAG	Reverse primer for qPCR
SLC2A3-F	GCGGGTGTGGTTAATACTATC	Forward primer for qPCR
SLC2A3-R	GCCCCAATACAGACAAAGC	Reverse primer for qPCR
ARHGAP24-F	TGCACAGTTTAGTTTCCAGC	Forward primer for qPCR
ARHGAP24-R	GAACTTTTTCCTCTCCTGATCC	Reverse primer for qPCR
HIST1H4K-F	AAGTACTGCGCGACAATATC	Forward primer for qPCR
HIST1H4K-R	TCTCCAGGAACACCTTCAG	Reverse primer for qPCR
CDH1-F	ATGAGTGTCCCCCGGTATCTTC	Forward primer for qPCR
CDH1-R	CGGAACCGCTTCCTTCATAGTC	Reverse primer for qPCR
ZNF165-F	AGCAGTACTCCAGGTTCAAG	Forward primer for qPCR
ZNF165-R	TCACTCTCATTATCACAGTCCC	Reverse primer for qPCR
LSD1-F	GCTCGGGGCTCTTATTCCTA	Forward primer for qPCR
LSD1-R	CCCAAAAACTGGTCTGCAAT	Reverse primer for qPCR
TNFSF18-F	GTTGCTATTTCTTTGCTCCTTC	Forward primer for qPCR
TNFSF18-R	CCAGTCAGACACCTTATTCAC	Reverse primer for qPCR
RAB25-F	CGTGGGTAACAAAAGTGACC	Forward primer for qPCR
RAB25-R	CTAGCTCAACATTGGTAGAGTC	Reverse primer for qPCR
GAPDH-F	GAAGGTGAAGGTCGGAGTC	Forward primer for qPCR
GAPDH-R	GAAGATGGTGATGGGATT	Reverse primer for qPCR
VAT1L-ChIP-F7	ACATTCAACAGGAGGAACCC	Forward primer for qPCR for ChIP
VAT1L-ChIP-R7	TTTGACGCGGATCTTGAGC	Reverse primer for qPCR for ChIP
VIM-ChIP-F8	GCTGTAAGTTGGTAGCACTGA	Forward primer for qPCR for ChIP
VIM-ChIP-R8	TTCTGTCGAGGGACCTAACG	Reverse primer for qPCR for ChIP
IFI6-ChIP-F3	TGGTGATCAGGCTTCACTAAG	Forward primer for qPCR for ChIP
IFI6-ChIP-R3	CTGCAGTTTCATTTTCCCCTC	Reverse primer for qPCR for ChIP
IL8-ChIP-F3	GATCTTGTTCTAACACCTGCC	Forward primer for qPCR for ChIP
IL8-ChIP-R3	GCAAACCTGAGTCATCACAC	Reverse primer for qPCR for ChIP
p21-ChIP-F1	GGGGCGGTTGTATATCAGG	Forward primer for qPCR for ChIP
p21-ChIP-R1	GGCTCCACAAGGAACTGACT	Reverse primer for qPCR for ChIP
p21-ChIP-F2	CTCTCCAATTCCCTCCTTCC	Forward primer for qPCR for ChIP
p21-ChIP-R2	AGAAGCACCTGGAGCACCTA	Reverse primer for qPCR for ChIP

Received 28 August 2012/15 October 2012; accepted 17 October 2012
Published as BJ Immediate Publication 17 October 2012, doi:10.1042/BJ20121360